Structure−Function Analysis of the Mammalian DNA Polymerase β Active Site: Role of Aspartic Acid 256, Arginine 254, and Arginine 258 in Nucleotidyl Transfer

Karen L. Menge, Zdenek Hostomsky, Beverly R. Nodes, Geoffrey O. Hudson, Soheil Rahmati, Ellen W. Moomaw, Robert J. Almassy, and Zuzana Hostomska*

Agouron Pharmaceuticals, Inc., 3565 General Atomics Court, San Diego, California 92121

Received August 18, 1995; Revised Manuscript Received October 11, 1995[⊗]

ABSTRACT: The crystal structure of the catalytic domain of rat DNA polymerase β revealed that Asp256 is located in proximity to the previously identified active site residues Asp190 and Asp192. We have prepared and kinetically characterized the nucleotidyl transfer activity of wild type and several mutant forms of human and rat pol β. Herein we report steady-state kinetic determinations of K_m^{dTTP}, $K_m^{(dT)_{16}}$, and k_{cat} for mutants in residue Asp256 and two neighboring residues, Arg254 and Arg258, all centrally located on strand β7 in the pol β structure. Mutation of Asp256 to alanine abolished the enzymatic activity of pol β. Conservative replacement with glutamic acid (D256E) led to a 320-fold reduction of k_{cat} compared to wild type. Replacement of Arg254 with an alanine (R254A) resulted in a 50-fold reduction of k_{cat} compared to wild type. The $K_m^{(dT)_{16}}$ of D256E and R254A increased about 18-fold relative to wild type. Replacement of Arg254 with a lysine resulted in a 15-fold decrease in k_{cat}, and a 5-fold increase in the $K_m^{(dT)_{16}}$. These kinetic observations support a role of Asp256 and Arg254 in the positioning of divalent metal ions and substrates in precise geometrical orientation for efficient catalysis. The mutation of Arg258 to alanine (R258A) resulted in a 10-fold increase in K_m^{dTTP} and a 65-fold increase in $K_m^{(dT)_{16}}$ but resulted in no change of k_{cat}. These observations are discussed in the context of the three-dimensional structures of the catalytic domain of pol β and the ternary complex of pol β, ddCTP, and DNA.

DNA polymerase β (pol β)[1] is one of five known mammalian DNA polymerases (Wang, 1991). Pol β has been implicated in a variety of mammalian DNA repair mechanisms (Matsumoto & Bogenhagen, 1989; Wiebauer & Jiricny, 1990; Dianov et al., 1992). Recently, it was reported that pol β catalyzes the release of 5′-terminal deoxyribose phosphate residues from incised apurinic−apyrimidinic sites (Matsumoto & Kim, 1995). The physical association of polymerase and excision activities on one protein may enhance the efficiency of nucleotide excision repair. The 335 amino acids of pol β form two domains that are linked by a protease-sensitive region. The N-terminal 8 kDa domain has been implicated in template binding and deoxyribose phosphate excision, while the C-terminal 31 kDa domain contains the polymerase catalytic site (Kumar et al., 1990a,b; Matsumoto & Kim, 1995). The pol β-catalyzed nucleotidyl transfer activity requires divalent metal ions and proceeds via a two-step ordered kinetic mechanism (Tanabe et al., 1979). The small size and functional simplicity of pol β make it an attractive model for the structure−function study of a nucleotidyl transfer mechanism in template-directed polymerization of nucleic acids.

Pol β shares 24% amino acid identity and 22% conservative substitutions with terminal deoxynucleotidyltransferase (Matsukage et al., 1987) but has limited sequence similarity with other nucleic acid polymerases. Delarue et al. (1990) aligned amino acid sequences of all known polymerases and correlated this information with the three-dimensional structure of the Klenow fragment of DNA polymerase I (KF), the only structurally characterized polymerase at that time. Several sequence motifs were identified (designated A, B, and C) that contain conserved amino acid residues. Motif C contains two acidic residues located in a β hairpin−turn while motif A contains a strictly conserved aspartic acid, located away from motif C in the primary structure. In the overall three-dimensional arrangement the three acidic residues of motifs A and C are juxtaposed to form the carboxylate triad implicated in divalent metal binding at the active site. This correlation of polymerase sequence with important structural arrangement was reinforced when the crystal structure of HIV-1 reverse transcriptase (RT) revealed that active site regions in KF and RT could be superimposed (Kohlstaedt et al., 1992; Jacobo-Molina et al., 1993).

The sequence alignment predicted that acidic amino acids of motif C in KF (Asp882 and Glu883) and RT (Asp185 and Asp186) would correspond to Asp190 and Asp192 of pol β while the aspartic acid of motif A (Asp705 in KF and Asp110 in RT) would correspond to Asp17 in pol β. Mutations of carboxylate residues in motifs C and A of RT (Larder et al., 1987; Hostomsky et al., 1992; Boyer et al., 1992) or KF (Polesky et al., 1990, 1992) resulted in severe loss of polymerase activity, indicating these residues are important in catalysis. Similarly, in pol β, mutation of Asp190 and Asp192 (motif C) also resulted in severe loss of catalytic activity (Date et al., 1991), indicating the alignment was correct in predicting Asp190 and Asp192 as catalytically important residues.

When the high-resolution crystal structure of the catalytic domain of pol β became available (Davies et al., 1994; Sawaya et al., 1994), it revealed that although pol β has an

* Corresponding author. Phone: (619) 622-7917. FAX: (619) 622-7998. E-mail: zha@agouron.com.

[⊗] Abstract published in *Advance ACS Abstracts,* December 1, 1995.

[1] Abbreviations: pol β, DNA polymerase β; KF, Klenow fragment of *Escherichia coli* DNA polymerase I; RT, HIV-1 reverse transcriptase.

0006-2960/95/0434-15934$09.00/0

overall U shape reminiscent of other polymerase structures (KF, Ollis et al., 1985; RT, Kohlstaedt et al., 1992, and Jacobo-Molina et al., 1993; and T7 RNA polymerase, Sousa et al., 1993), its folding topology is unique, suggesting that pol β does not share a common ancestor with these other three structurally characterized polymerases. In particular, the β strand that provides the third carboxylate residue to the pol β catalytic site runs in the opposite direction than the strand corresponding to motif A in KF and RT. From the pol β crystal structure, Asp190 and Asp192 were structurally confirmed as active site residues and Asp256 was proposed as the third member of the carboxylate triad at the polymerase active site.

In addition to localizing Asp256 to the pol β active site, the structure of the catalytic domain identified other amino acids of potential importance in pol β-catalyzed nucleotidyl transfer. In the absence of a DNA substrate, the side chains of Asp192 and Asp256 do not interact directly with the metal ions. Instead, they form salt bridges with arginine residues symmetrically located on each side of Asp256 along the strand β7 (Davies et al., 1994). Asp192 forms a salt bridge with Arg258 and Asp256 with Arg254, while two manganese ions are coordinated by Asp190. In this report, we explore the potential significance of this particular arrangement of functional groups in the catalytic site of pol β. We expressed, purified, and kinetically characterized recombinant forms of pol β containing mutations in Asp17, Asp256, Arg254, and Arg258. The results of the site-directed mutagenesis and kinetic analysis are discussed in the context of the high-resolution structure of the catalytic domain of pol β as well as the recently solved structure of the ternary complex of pol β, ddCTP, and DNA (Pelletier et al., 1994; Almassy et al., unpublished results).[2]

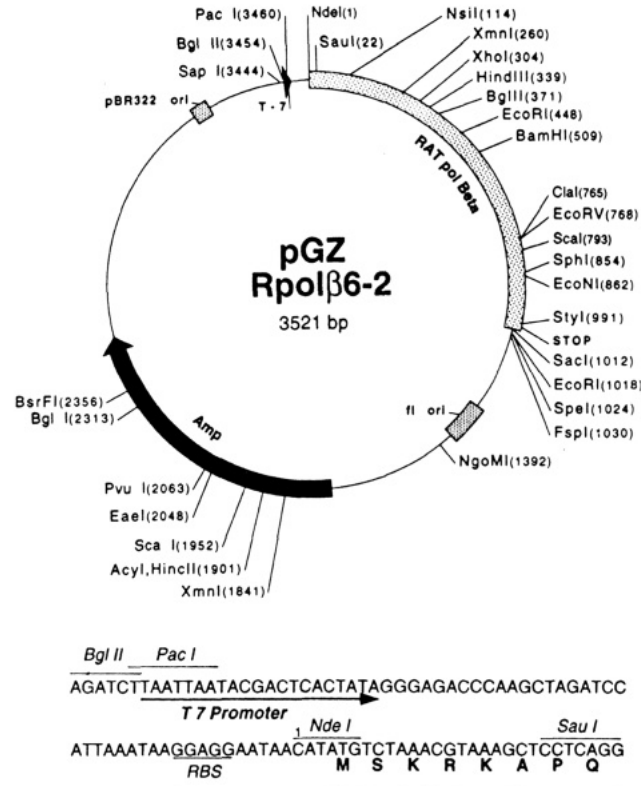

FIGURE 1: Map of the construct pGZ/Rpol β6-2 used for expression and mutagenesis of rat DNA polymerase β. The sequence of the synthetically prepared *Bgl*II−*Sau*I segment containing signals for efficient transcription and translation of pol β in *E. coli* is shown in detail. The *Sau*I−*Sac*I portion of the pol β gene corresponds to a naturally occurring sequence amplified from a rat cDNA library. The nucleotide sequence numbering of this construct starts with the first C of the unique *Nde*I site.

MATERIALS AND METHODS

Materials. Oligo(dT)$_{16}$ and poly(dA)$_{300}$ were from Pharmacia LKB Biotechnology, Inc. Concentrations of oligo- and polynucleotides were determined by absorption at 260 nm and are reported as molecular (not total nucleotide) concentrations. ^{32}P-Labeled nucleoside triphosphates were from DuPont NEN. All chemicals were of analytical grade.

Cloning of Human and Rat DNA Polymerase β. A DNA sequence encoding DNA polymerase β was amplified from a human testis cDNA library (Clontech) and a rat brain cDNA library (Clontech) using oligonucleotides DPBM3 (5′-AAACGGAAGGCGCCTCAGGAGACTCTCAACGG) and DPBC2 (5′-GGAATTCGAGCTCATTATTCGCTCCGGTC-CTTGGG) as primers for the PCR reaction. The primers were designed on the basis of the published sequences of rat and human cDNA clones (Zmudzka et al., 1986; SenGupta et al., 1986; Matsukage et al., 1987). The DPMB3 primer introduced a G to T change in codon 7 to create a unique *Sau*I site. The amplified sequences were inserted as *Sau*I−*Sac*I fragments into a multicopy expression vector, pGZ. This vector was constructed by replacing the lac Z′ portion of the phagemid pTZ18R (Mead et al., 1986) with a synthetic segment containing a consensus ribosomal binding site (RBS), followed by sequence coding for the N-terminal seven amino acids of pol β under the control of the Φ 10 promoter of phage T7. This sequence, corresponding to the *Nde*I−*Sau*I portion of the pol β gene, had codons modified for efficient initiation of translation in *Escherichia coli*.

The resulting constructs [pGZ/Dpol β7-2 with human pol β and pGZ/Rpol β6-2 with rat pol β gene (Figure 1)] were induced for expression in *E. coli* K12 strain AP 401(k) by infection with phage mGP1-2 (gift from S. Tabor), an M13 derivative that carries the gene for T7 RNA polymerase under the control of lac promoter, essentially as described (Hostomsky et al., 1989). For pGZ/Rpol β6-2 the temperature of the bacterial culture upon induction was lowered to 30 °C to increase the solubility of rat pol β.

Site-Directed Mutagenesis of Pol β. The mutant forms of pol β were generated using the Transformer mutagenesis kit (Clontech) essentially as suggested by the manufacturer, except that single-stranded plasmids rather than double-stranded plasmids were used as templates. The single-stranded forms of the plasmids were produced by superinfection of the *E. coli* strain XL-1 (blue) harboring pGZ/Dpol β7-2 or pGZ/Rpol β6-2 with the helper phage M13K07 and purified using the ssPhage DNA isolation kit (BIO 101). Following the annealing of mutagenic and selection primers, the second strand was synthesized using T4 DNA polymerase. Upon treatment with T4 DNA ligase, the DNA was used directly for transformation of the *E. coli* strain BMH 71-18 *mutS*. The mixed plasmid preparation was digested with a selection restriction enzyme (*Bgl*I or *Eco*RV) and

[2] The structures of the pol β catalytic domain of Davies et al. (1994, Brookhaven Protein Data Bank entry 1rpl) and the pol β ternary complex structure of Almassy et al. (unpublished results, see Figure 5 legend) and the ternary structure of Pelletier et al. (1994, Brookhaven Protein Data Bank entry 2bpf) were used in our analysis.

transformed into the *E. coli* strain XL-1 (blue). The presence of mutations in individual clones was verified by DNA sequencing. The mutant pol β proteins were expressed as described above for wild-type pol β.

Purification of Wild-Type and Mutant DNA Polymerase β. The wild-type and mutant proteins were purified from approximately 100 g of cell paste by the procedure presented here. Throughout purification, pol β was detected by nucleotidyl transfer activity or SDS−PAGE. All steps were carried out at 4 °C. Cell paste was resuspended in 1 mL of buffer A (50 mM Tris-HCl, pH 7.5, 10% glycerol, 0.5 M KCl, 0.1 mM EDTA, 1 mM DTT, and 1 mM PMSF) for every 0.87 g of cells. The cells were microfluidized, brought to 0.5% NP40, 0.8 M KCl, and 2 mM PMSF, and held on ice for 30 min. The crude lysate was clarified by centrifugation in a SS34 rotor at 15K rpm for 45 min. The cleared lysate was diluted 2-fold with buffer B (50 mM Tris-HCl, pH 7.5, 10% glycerol, 0.1 mM EDTA, and 1 mM DTT) and applied to a 160 mL DEAE-Sephacryl column equilibrated with buffer A. The column was washed with buffer A at a flow rate of 2.2 mL/min, and 18 mL fractions were collected. The flow-through fractions containing pol β were pooled and dialyzed against buffer C (50 mM Tris-HCl, pH 7.5, 10% glycerol, 0.2 M KCl, 0.1 mM EDTA, and 1 mM DTT) with Spectra/Por 8000 dialysis tubing. The dialyzed pool was applied to a 300 mL phospho-cellulose (Whatman P11) column equilibrated in buffer C at a flow rate of 2.5 mL/min. Loading was followed by a 1200 mL linear gradient of buffer C from 0.2 M KCl to 1.25 M KCl, and 18 mL fractions were collected. Wild-type and mutant DNA polymerase β proteins eluted from the column at 0.75 M KCl. The cleanest fractions of the pol β peak as judged by SDS−PAGE were pooled and dialyzed against buffer D (50 mM sodium acetate, pH 6.0, and 1 mM DTT) with Spectra/Por 8000 dialysis tubing. The white precipitate formed during dialysis was removed by centrifugation in a SS34 rotor at 10K rpm for 10 min. Half of the supernatant at a time was applied to an 8 mL MonoS column (Pharmacia FPLC) equilibrated in buffer D, and a linear gradient of buffer D from 0 to 1 M NaCl was run at 3 mL/min and 3 mL fractions were collected. Wild-type and mutant DNA polymerase β proteins eluted from the column at 0.5 M NaCl. Fractions of the pol β peak judged pure SDS−PAGE were pooled and dialyzed against one of several buffers: human wild type and human D17A with 25 mM Tris-HCl, pH 7.5, and 1 mM DTT; rat wild type with 50 mM HEPES, pH 7.5, 1 mM DTT, and 50 mM NaCl; rat D256A, rat D256E, rat R258A, rat R254A, rat R254K, and the switch mutant rat R254D/D256R with 100 mM Tris-HCl, pH 7.0, and 10 mM ammonium sulfate. All listed buffers were found equally suitable for storage of these proteins. Dialyzed protein samples were concentrated to greater than 12 mg/mL and were stored at −70 °C. Concentration of pol β was determined by absorption at 280 nm and the theoretical extinction coefficients of 23.6 mM^{-1} cm^{-1} for wild type and mutant human pol β and 22.2 mM^{-1} cm^{-1} for wild type and mutant rat pol β.

Polymerase Activity Assay. Nucleotidyl transfer activity of wild-type and mutant pol β was followed by incorporation of [^{32}P]dTMP to an oligo(dT)$_{16}$ primer and poly(dA)$_{300}$ template at 37 °C. Standard polymerase reaction mixes (40−50 μL) contained the following: 50 mM Tris-HCl (pH 7.8); 70 mM KCl; 1 mM DTT; 100 μg/mL BSA; 5% glycerol; 2 mM $MnCl_2$; and protein, dTTP, [α-^{32}P]dTTP (125−5000 dpm/pmol), and oligo(dT)$_{16}$ primer, and poly(dA)$_{300}$ template. Mn^{2+} was chosen as the divalent metal ion in our analysis as under these assay conditions Mn^{2+} is preferred over Mg^{2+} (Menge et al., unpublished observations). Protein concentrations ranged from 10 to 60 nM for wild type and from 4 nM to 1.25 μM for mutant pol β depending on activity. The $K_m^{(dT)_{16}}$ was determined by titrating (dT)$_{16}$ over a range inclusive of K_m in the presence of saturating concentrations of dTTP. Similarly, the K_m^{dTTP} was determined by titrating dTTP over a range inclusive of K_m in the presence of saturating concentrations of (dT)$_{16}$. The concentration of (dA)$_{300}$ was held constant for each titration and was always such that at least 150 bases of each (dA)$_{300}$ strand were available as template. Reactions were initiated by the addition of dTTP after preincubation of all other components at 37 °C for 10 min. Free Mn^{2+} concentration was held constant by including a 1:1 ratio of dTTP:$MnCl_2$ in dTTP used to initiate reactions. Time points (5 μL) at 20 or 30 s intervals were quenched in 25 mM EDTA (45 μL) and held on ice.

Incorporation of [^{32}P]dTMP into the primer strand was measured using the following procedure which results in separation of unincorporated from incorporated [^{32}P]dTMP at high throughput. A 96-well microfiltration apparatus (Bio-Rad Bio-Dot SF) was fitted with a NA45 DEAE-cellulose membrane (Schleicher & Schuell) that was prepared by 10 min washes in 100 mM EDTA, 3 times in 1 M NaCl, and then briefly in 0.5 M NaOH followed by extensive rinsing with water. Sets of 9−16 quenched time points (45 μL) were applied to individual wells of the apparatus, house vacuum was applied, and the wells were washed with 4 × 100 μL of 0.3 M ammonium formate (pH 8.0), allowing complete drainage between washes. After all sets of time points were applied and washed, the filter was removed from the apparatus and an additional 10 min wash with 0.3 M ammonium formate with agitation was carried out (Bryant et al., 1983). The washed filter was air-dried after a quick rinse in EtOH and wrapped in plastic wrap. On a separate filter, 3 × 2 μL of quenched time points from each reaction were spotted and used for the calibration of total dTTP. The air-dried filter was wrapped in plastic wrap, and both filters were exposed to a PhosphorStorage plate for 1−2 h. The PhosphorStorage plate was developed using a Molecular Dynamics PhosphorImager, Model SF. Quantitative analysis was carried out using the ImageQuant software provided with the PhosphorImager.

Determination of Kinetic Parameters. The DNA polymerase β nucleotidyl transfer reaction proceeds via an ordered two-step mechanism in which DNA binds first followed by dNTP binding and catalysis (Tanabe et al., 1979). Kinetic parameters (K_m^{dTTP}, $K_m^{(dT)_{16}}$ and k_{cat}) were approximated by titrating one substrate over a range inclusive of K_m in the presence of saturating concentrations of the other substrate. Reactions carried out under these conditions lead to a hyperbolic dependence of initial rate (V_i) on the concentration of the varied substrate that was amenable to standard Michaelis−Menten analysis of a single substrate reaction. Initial velocities (V_i) were determined using linear regression on the time courses obtained as described above and were normalized to the pol β concentration used in the reaction. Eadie−Hofstee plots (V_i vs V_i/[substrate]) were constructed from dTTP titrations and (dT)$_{16}$ titrations and

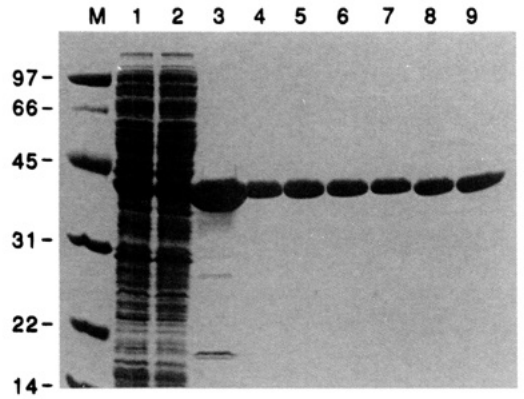

FIGURE 2: Coomassie-stained SDS−15% polyacrylamide gel: (lane M) Bio-Rad low-range molecular weight markers; (lanes 1−3) purification steps of rat R258A, (lane 1) 2.5 μL of crude lysate; (lane 2) 5 μL of DEAE pool; (lane 3) 10 μL of phosphocellulose pool; (lanes 4−9) 4 μg of MonoS pooled and concentrated rat wild-type pol β, rat D256E, rat R254A, rat R258A, human wild-type pol β, and human D17A.

were used to estimate K_m^{dTTP} and $K_m^{(dT)_{16}}$, respectively. The y-intercept of the least squares fit of the Eadie−Hofstee data represents k_{cat} while the slope is negative K_m. Unless otherwise indicated, titration of dTTP or $(dT)_{16}$ for a given protein resulted in the same k_{cat} value, an indication that saturation of the substrate held constant was achieved. Each determination of kinetic parameters was repeated at least one time.

RESULTS

Protein Purification. The DNA polymerase β genes from rat and human cDNA libraries were cloned as described in Materials and Methods. Site-directed mutagenesis was used to construct the following mutant proteins: human D17A, rat D256A, rat D256E, rat R254A, rat R254K, rat R258A, and the switch mutant rat R254D/D256R. Full sequence analysis of the mutated genes indicated changes only in the targeted region. Wild-type and mutant proteins were purified by microfluidization, DEAE-Sephacryl column chromatography, phosphocellulose column chromatography, and MonoS FPLC as described in Materials and Methods. Wild-type rat pol β purified by this procedure was previously used in crystallographic determination of the catalytic domain structure (Davies et al., 1994). An SDS−PAGE analysis of the steps of purification of rat R258A is shown in Figure 2 along with the final purified samples of wild-type rat pol β, rat D256E, rat R254A, rat R258A, wild-type human pol β, and human D17A. SDS−PAGE analysis demonstrated that the altered proteins rat D256A, rat R254K, and the switch mutant rat R254D/D256R were similarly pure (data not shown). Mutant proteins responded as wild type throughout purification and yielded at least 2 mg of protein/g of wet cell paste.

Kinetics of Polymerase Activity of Rat and Human Wild-Type DNA Polymerase β. Rat and human DNA polymerase differ at 16 positions, 15 of which are located in the C-terminal catalytic domain of the protein. To determine if these differences affect the properties of the nucleotidyl transfer activity, rat and human pol β were kinetically characterized using substrates oligo$(dT)_{16}$ primer, poly$(dA)_{300}$ template, and incoming nucleotide dTTP. The dependence of the initial velocity (V_i) of rat and human polymerase β-catalyzed nucleotidyl transfer on dTTP concentration was measured at a fixed, saturating concentration of $(dT)_{16}$ primer, and representative titrations are shown in Figure 3A,B (upper

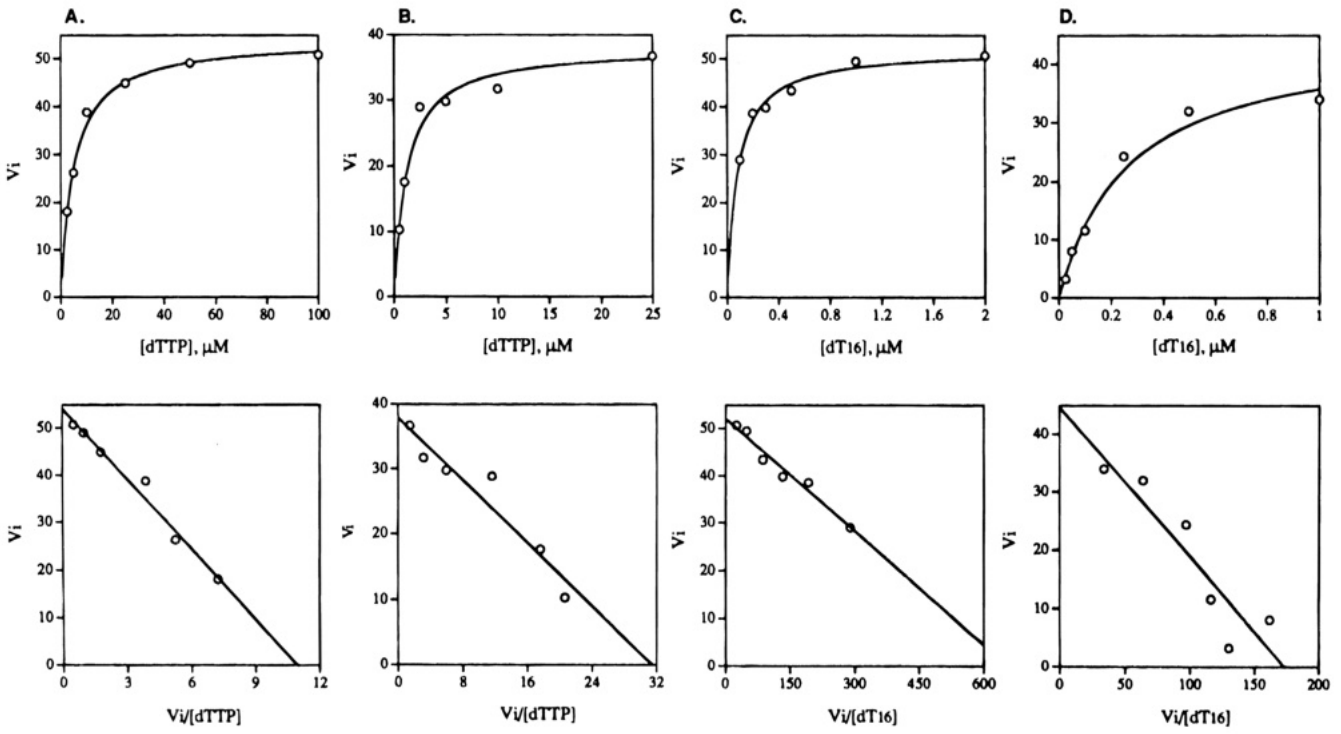

FIGURE 3: Initial velocity (upper panel) and Eadie−Hofstee (lower panel) plots of rat and human wild-type pol β dTTP and $(dT)_{16}$ titrations. V_i (min^{-1}) represents the initial rate measured normalized to the concentration of pol β in the reaction. Panels: (A) dTTP titration at 59 nM rat pol β, 5 μM $(dT)_{16}$, and 0.5 μM $(dA)_{300}$; (B) dTTP titration at 12 nM human pol β, 5 μM $(dT)_{16}$, and 0.5 μM $(dA)_{300}$; (C) $(dT)_{16}$ titration at 59 nM rat pol β, 100 μM dTTP, and 0.5 μM $(dA)_{300}$; (D) $(dT)_{16}$ titration at 12 nM human pol β, 10 μM dTTP, and 0.5 μM $(dA)_{300}$. The points on the initial velocity plots are the observed data for a single titration while the curve was generated from K_m and k_{cat} determined in the Eadie−Hofstee analysis using the Michaelis−Menten velocity equation for single substrate reactions.

Table 1: Kinetic Parameters of the Nucleotidyl Transfer Activity of Wild-Type and Mutant Pol β[a]

protein	K_m^{dTTP}, μM		$K_m^{dT_{16}}$, μM		k_{cat}, min^{-1}	
	av	range[b]	av	range	av	range
rat wt	4.7	4.5−4.9 (2)	0.09	0.08−0.1 (3)	51	39−67 (5)
rat D256A[c]					ND[d]	
rat D256E	2.2	2.1−2.4 (2)	1.5	1.3−1.8 (2)	0.16	0.11−0.21 (4)
rat R254A	2.5	2.1−2.8 (2)	1.7	1.6−1.8 (2)	1	0.7−1.1 (0.4)
rat R254K	1.0	0.9−1.1 (2)	0.48	0.45−0.51 (2)	3.4	2.7−4.3 (4)
rat R254D/D256R					ND	
rat R258A	46	37−55 (3)	6	3.9−8.4 (3)	72	50−100 (6)
human wt	1.2	1.2−1.2 (2)	0.4	0.2−0.6 (3)	42	28−51 (5)
human D17A	0.7	0.42−1.2 (3)	0.1	0.11−0.12 (2)	34	24−56 (5)

[a] See text for experimental details. [b] The average value is reported along with the observed range. The number of independent determinations is given in parentheses. [c] In addition to standard conditions, polymerase activity of D256A was not detectable with Mg^{2+} at pH 7.8 or with either Mg^{2+} or Mn^{2+} at pH 8.8. [d] ND, activity not detectable.

panel). The points in Figure 3A,B (upper panel) represent the observed data while the curves were simulated using the K_m^{dTTP} and k_{cat} values estimated from linear regression of the Eadie−Hofstee analysis (Figure 3A and 3B, lower panel) substituted into the Michaelis−Menten equation for a single substrate reaction. This figure represents single titrations while the summarized data in Table 1 represent average values of at least two independent determinations. The analogous plots for the titration of $(dT)_{16}$ at a fixed, saturating concentration of dTTP for rat and human pol β are also displayed in Figure 3C,D. The K_m^{dTTP} and $K_m^{(dT)_{16}}$ for rat pol β were 4.7 and 0.09 μM, respectively, and the K_m^{dTTP} and $K_m^{(dT)_{16}}$ for human pol β were 1.2 and 0.4 μM, respectively. The differences between K_m values for the rat and human pol β are not large, a 4-fold increase of K_m^{dTTP} for rat pol β relative to human pol β and a 4-fold increase of $K_m^{(dT)_{16}}$ for human pol β relative to rat pol β. The k_{cat} for rat pol β was 51 min^{-1} while that for human pol β was 42 min^{-1}. The observed range of the k_{cat} for rat and human pol β overlapped, indicating that the k_{cat} of rat pol β is experimentally identical to that of human pol β. Our observed kinetic parameters for recombinant pol β are in agreement with those previously reported for pol β isolated from human liver and mouse myeloma (Wang et al., 1977; Tanabe et al., 1979).

The lack of a large difference between rat and human DNA polymerase β in the nucleotidyl transfer reaction is not surprising since 11 of the 15 residues that vary between rat and human pol β in the catalytic domain are on the protein surface. The 4 that are on the interior of the protein are not near the supposed active site. Since pol β from rat and human are essentially identical in the nucleotidyl transfer reaction, the effects of site-directed changes made in either human or rat pol β are assumed to reflect the general properties of DNA polymerase β.

Kinetics of Polymerase Activity of Rat and Human Mutant DNA Polymerase β. The kinetic parameters for the mutant proteins were determined using the same method described above for wild-type pol β. The sequence alignment of polymerases predicted that Asp17 might be involved in pol β-catalyzed nucleotidyl transfer. Replacement of Asp17 with an alanine (D17A) in human pol β resulted in a protein with a K_m^{dTTP} of 0.7 μM, a $K_m^{(dT)_{16}}$ of 0.1 μM, and a k_{cat} of 34 min^{-1} (Table 1). These observed values represent a 4-fold or less change in K_m and no experimental difference in k_{cat} compared to human wild-type pol β. This indicates that Asp17 is not required for the nucleotidyl transfer activity of pol β.

The three-dimensional structure of the catalytic domain of pol β revealed that Asp256 is in proximity to the supposed active site of pol β (Davies et al., 1994). To ascertain the importance of Asp256 in pol β-catalyzed nucleotidyl transfer, Asp256 was changed to an alanine residue (D256A). The D256A protein was not active in the nucleotidyl transfer assay over a range of conditions examined (Table 1). However, D256A retained wild-type-level DNA binding as measured by a gel mobility shift assay (data not shown), indicating that the protein is properly folded. Conservative replacement of Asp256 with a glutamic acid (D256E) resulted in a protein with severe, but not total loss of catalytic activity with the k_{cat} displaying a 320-fold reduced rate of 0.16 min^{-1} (0.3% of wild type). The K_m^{dTTP} was not significantly affected, with a 2-fold decrease to 2.2 μM relative to wild type. However, the $K_m^{(dT)_{16}}$ at 1.5 μM was increased 17-fold (Table 1).

In the structure of the catalytic domain, Asp256 forms a salt bridge with Arg254 and Asp192 forms a salt bridge with Arg258. To examine the roles of Arg254 and Arg258 in pol β function, these two arginine residues were targeted for site-directed mutagenesis. Three mutant proteins were prepared in which the arginine was replaced with alanine (R254A and R258A) or lysine (R254K). Replacement at Arg254 led to proteins with reduced enzymatic capacity as indicated by a reduction in k_{cat} to 1 min^{-1} (2% of wild type) and 3.4 min^{-1} (7% of wild type) for R254A and R254K, respectively. The K_m^{dTTP} for R254A at 2.5 μM was not significantly affected by the mutation while the $K_m^{(dT)_{16}}$ for R254A was increased 19-fold over wild-type to 1.7 μM (Table 1). The K_m^{dTTP} for R254K was reduced 5-fold relative to wild type to 1 μM, and the $K_m^{(dT)_{16}}$ was increased 5-fold relative to wild-type to 0.48 μM (Table 1). Replacement of Arg258 with an alanine (R258A) resulted in a protein with a 65-fold increase in $K_m^{(dT)_{16}}$ to 6 μM. The K_m^{dTTP} for R258A also increased to 46 μM, which is 10-fold above the value measured for wild type. The k_{cat} of 72 min^{-1}, however, was not significantly different from that observed for wild type (Table 1).

Steady-state kinetic analysis allows prediction of the potential role of amino acids in enzyme function. Although the k_{cat} and K_m values determined from a steady-state analysis represent a compilation of individual rate constants along the reaction pathway, a site-directed mutation resulting in a k_{cat} change is generally interpreted as the targeted amino acid playing a role in catalysis while a mutation resulting in a change in K_m is generally interpreted as a role for the targeted amino acid in the binding of substrate(s). In our experi-

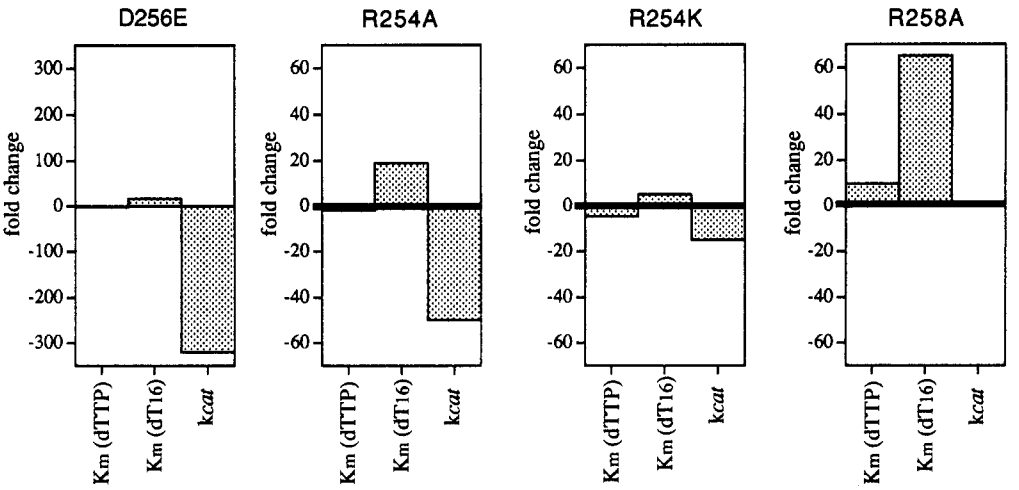

FIGURE 4: Relative changes of K_m^{dTTP}, $K_m^{(dT)_{16}}$, and k_{cat} of D256E, R254A, R254K, and R258A. Parameters are represented as "fold changes" relative to the value of wild-type rat pol β. An increase is displayed as a positive fold change while a decrease is displayed as a negative change. Zero represents no change. Note that D256E is plotted on a different scale than R254A, R254K, and R258A.

mental system $(dT)_{16}$ binding is dependent on interactions between primer and protein, template and protein, and template and primer. Hence the $K_m^{(dT)_{16}}$ reflects both primer and template binding. Furthermore, the template strand of the DNA substrate provides contacts for binding of the incoming deoxyribonucleotide. Thus a change in template binding caused by a site-directed mutation may be reflected in a change in both the K_m^{dTTP} and $K_m^{(dT)_{16}}$.

The removal of the acidic side chain at position 256 resulted in a catalytically inactive protein (D256A). This indicates that Asp256 is essential to the enzymatic action of pol β. Substitution of Asp256 to a glutamate or substitution of Arg254 to an alanine or lysine had similar patterns of effects on the kinetic parameters (Figure 4). D256E, R254A, and R254K all display a decrease in k_{cat} and an increase in $K_m^{(dT)_{16}}$ relative to wild type. In all three cases, the relative decrease in k_{cat} was greater than the relative increase in $K_m^{(dT)_{16}}$. Additionally, the change in K_m^{dTTP} for these three proteins was relatively small. This suggests that both Arg254 and Asp256 contribute to catalysis and to primer/template binding. Since Asp256 and Arg254 are in salt bridge contact in the catalytic domain structure, we attempted to switch the amino acids at these two positions (R254D/D256R). The protein R254D/D256R was not active, indicating the importance of the arrangement of Arg254 and Asp256 in the active site (Table 1). Substitution of Arg258 with an alanine resulted in a completely different pattern of effects on the kinetic parameters (Figure 4). The R258A protein retained wild-type-level k_{cat} while showing a striking increase in the K_m for both substrates. These results suggest a role for Arg258 in the binding of substrates but not in a catalytic step of pol β-catalyzed nucleotidyl transfer. The structure–function relationship of the side chains at positions 254, 256, and 258 is explored in the context of the three-dimensional structure of pol β in the Discussion.

DISCUSSION

Sequence alignment of polymerases (Delarue et al., 1990) based on the known structural elements of KF identified three motifs of potential importance in polymerase-catalyzed activities. Two of these motifs, A and C, define a triad of acidic residues that comprise the polymerase active site. In pol β, the sequence alignment predicted Asp17, Asp190, and Asp192 as the acidic amino acids of motif A and C. Mutations of Asp190 or Asp192 to serine were previously shown to result in a loss of catalytic activity (Date et al., 1991), supporting the assignment of 190 and 192 to the active site of pol β. Herein we demonstrated that replacement of Asp17 with alanine did not affect the catalysis of nucleotidyl transfer; thus Asp17 is not a member of the polymerase active site.

The recently reported structure of the catalytic domain of pol β by our group (Davies et al., 1994) as well as by Sawaya et al. (1994) provided insight into the active site arrangement in this enzyme. Pol β shares a similar overall shape with the other three polynucleotide-synthesizing proteins whose structures have been determined: KF (Ollis et al., 1985), RT (Kohlstaedt et al., 1992; Jacobo-Molina et al., 1993), and T7 RNA polymerase (Sousa et al., 1993). The polymerase domains in these enzymes contain three subdomains described as the fingers, palm, and thumb of a right hand (Kohlstaedt et al., 1992) that form a large cleft able to accommodate various primer/template substrates (Figure 5A). The active site acidic residues implicated in catalysis of nucleotidyl transfer are located in the palm subdomain. The superposition of the palm subdomain of RT, KF, and pol β revealed three carboxylate side chains situated in similar positions at the supposed active site. These residues correspond to Asp185, Asp186, and Asp110 of RT, Asp882, Glu883, and Asp705 of KF, as predicted from the sequence alignment, and Asp190, Asp192, and Asp256 of pol β. This superposition was the first indication that residue Asp256 may be involved in catalysis.

The importance of Asp256 in nucleotidyl transfer was verified by mutation of Asp256 to an alanine, which resulted in a complete loss of catalytic activity. Conservative replacement with glutamic acid (D256E) resulted in a protein with a k_{cat} of only 0.3% of that of wild-type pol β. Similar results were reported for Asp190 and Asp192 changed to glutamic acid (Date et al., 1991). Thus, the nucleotidyl transfer active site triad of pol β is defined by Asp190, Asp192, and Asp256.

The nucleotidyl transfer reaction catalyzed by DNA polymerases requires divalent metal ions for activity. Two divalent manganese ions were located near the acidic triad in the pol β structure of the catalytic domain soaked with

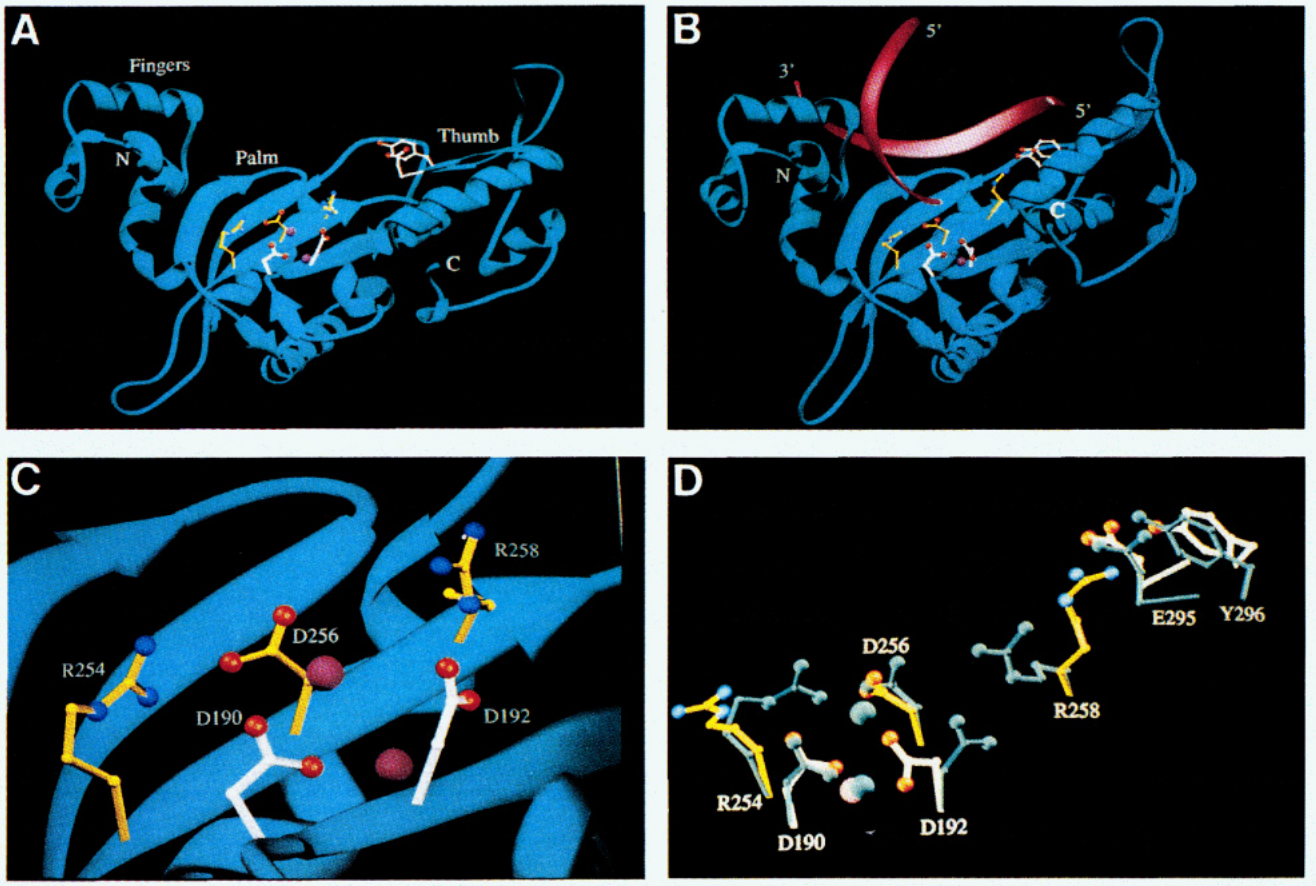

FIGURE 5: Ribbon representations of pol β (drawn using RIBBONS; Carson, 1991). (A) Overall fold of the catalytic domain of pol β. Three subdomains are labeled as fingers, palm, and thumb (Davies et al., 1994), and the N- and C-termini of the molecule are indicated. The side chains of amino acid residues analyzed in this work are displayed in yellow, and other important residues discussed in this work are in white. Two manganese ions are shown as purple spheres. (B) Overall fold of the pol β complexed with DNA (Almassy et al., unpublished results). DNA is shown in purple. The crystals of pol β complexed with an 11-mer and a 6-mer in the presence of ddCTP and magnesium were grown as described (Pelletier et al., 1994). The structure was solved by molecular replacement using entry 2bpf (Brookhaven Protein Data Bank). The view of the pol β DNA complex was attained by superposition of the backbone atoms of residues 180−212 of the palm subdomain of the catalytic domain in (A) with those of the pol β DNA complex. The 8 kDa domain was omitted for clarity. Note the movement of the thumb subdomain toward the catalytic site. (C) Close-up view of the nucleotidyl transfer catalytic site of pol β as in (A). Arg254, Arg258, and Asp256 are shown in yellow. The active site aspartic acids 190 and 192 are shown in white. (D) Movements of the side-chain positions of complexed (B) and uncomplexed (A) pol β. In gray are shown residues of pol β in the absence of the DNA substrate; in yellow and white are positions of side chains of residues in the ternary complex. Note the movement of Arg258 to the proximity of Glu295 and Tyr296.

$MnCl_2$ (Davies et al., 1994). The presence of two manganese ions in the active site of pol β agrees with the two-metal phosphoryl transfer mechanism proposed by Steitz and Steitz (1993). In this mechanism, the divalent metal ions are responsible for the chemistry of the polymerase reaction, while the role of the amino acids at the active site is to arrange the metal ions in a precise geometrical orientation relative to substrates for efficient catalysis. The observed effect on k_{cat} for Asp256, Asp190, and Asp192 mutants is consistent with this proposed role of the carboxylate triad. Increasing the side-chain length by one methylene group while maintaining the charge at position 190, 192, or 256 resulted in proteins with apparent reduced ability to arrange metals in an efficient catalytic orientation. The $K_m^{(dT)_{16}}$ for D190E, D192E, and D256E increased by the same magnitude relative to wild type (Table 1; Date et al., 1991), suggesting that these side chains may also function in substrate binding. Removal of any one of the acidic residues resulted in complete loss of catalytic activity, indicating that the three aspartic acid side chains act in concert to orient the divalent metal ions.

Residue Asp256 lies on the central strand (β7) of the five-stranded β sheet in the middle of the palm subdomain, within the symmetrical sequence RIDIR. In the catalytic domain structure, each arginine side chain forms a salt bridge with an active site residue, Arg254 with Asp256 and Arg258 with Asp192 (Figure 5C). The effects on k_{cat} and $K_m^{(dT)_{16}}$ of R254A and R254K were strikingly similar to those of active site aspartic acid to glutamic acid mutants. This suggests a role for Arg254 in the positioning of divalent metal and primer/template in the active site. In contrast, the k_{cat} of nucleotidyl transfer for R258A was the same as wild type. However, both the $K_m^{(dT)_{16}}$ and the K_m^{dTTP} were significantly increased compared to the wild type. The kinetic observations for R258A thus indicate that Arg258 does not participate in catalysis as would be suggested by the position of the Arg258 side chain in the catalytic domain structure. Instead, the increase in the K_m values suggests that Arg258 may be involved in substrate binding.

To expand on the structure−function role for Arg254 and Arg258, it is helpful to visualize pol β as a dynamic molecule. The nucleotidyl transfer reaction catalyzed by

polymerases consists of an ordered series of steps that seem to require an inherent structural flexibility for this class of enzymes. Multiple conformational states in RT, for example, have been inferred from kinetic studies (Johnson, 1993) as well as from comparison of several available crystal structures of RT (Jäger et al., 1994). Although a conformational change in pol β has not been biochemically tested, comparison of the uncomplexed catalytic domain structure (Davies et al., 1994; Sawaya et al., 1994) with the crystal structure of pol β complexed with DNA and dideoxynucleoside triphosphate (Pelletier et al., 1994; Almassy et al., unpublished results) provides structural evidence for a conformational isomerization that occurs upon substrate binding (Figure 5B). In the ternary complex, the oligonucleotides representing the DNA moiety are quite short and bind the protein with an opposing directionality when compared to KF or RT. Although questions have been raised regarding the physiological relevance of this pol β/DNA structure to serve as a prototype primer/template complex (Arnold et al., 1995), for the purpose of our study this structure is useful as an illustration of one of the possible conformational states of pol β that occurs along the nucleotidyl transfer pathway.

In the ternary complex, Asp256 is no longer in salt bridge contact with Arg254; instead, Arg254 is closer to the active site and forms an ion pair with Asp190 (Figure 5D). Asp190, in turn, is coordinated to a magnesium ion. Thus, Arg254 may serve to position Asp190 which then positions a magnesium ion. This may be the interaction that leads to the decrease in k_{cat} upon replacement of Arg254 with alanine or lysine. Additionally, Arg254 is in position to interact with the primer/template. The architecture of the active site in the substrate-bound structure of pol β supports the proposed function of Arg254 in the arrangement of the active site metals and in the positioning of the primer/template as suggested by the kinetic observations.

The salt bridge between Asp192 and Arg258 is not observed in the ternary complex. Instead, the side chain of Arg258 is moved 6 Å away from the active site and forms new intraprotein contacts: a salt bridge with Glu295 and a hydrogen bond with the phenol oxygen of Tyr296, both in the thumb subdomain (Figure 5D). The position of Arg258 in this substrate-bound structure is consistent with the observed equivalence of the k_{cat} of wild-type pol β and of R258A. In the complex, Arg258 does not interact directly with the incoming nucleotide or the primer/template. Although it is possible that the Arg258 side chain may interact with substrates along the reaction pathway, this conformation is not captured in the structure presented here. Alternatively, the increase in K_m values for R258A may be explained by Arg258-mediated interaction with the substrate. In the ternary complex, the thumb subdomain is moved closer to the palm region, appearing to close over the substrate binding site to form a productive substrate binding pocket (Figure 5B). Analogous motion of the thumb subdomain upon DNA binding was noticed also for KF (Beese et al., 1993) and RT (Jacobo-Molina et al., 1993). In addition to sharing a hydrogen bond with Arg258, Tyr296 contacts the primer/template in the pol β ternary structure. Thus, the interaction between Arg258 of the palm with Glu295 and Tyr296 of the thumb may contribute to protein−substrate interaction and to stabilization of a productive binding conformation of pol β. In the absence of the Arg258 side chain the thumb subdomain may not be stabilized in a position over the palm subdomain, resulting in an increase in the K_m values for R258A.

In summary, our kinetic data combined with pol β structural information leads us to the following scenario of nucleotidyl transfer catalyzed by DNA polymerase β. In the absence of substrate, Asp192 is in salt bridge contact with Arg258, and Asp256 with Arg254. Divalent metal ions bind to pol β via interaction with Asp190. Upon substrate binding, the salt bridges are broken. Arg254 moves closer to the active site, forms an ion pair with Asp190, and contributes to the positioning of active site metal ions. Additionally, Asp256 and Arg254 serve in the binding and positioning of the primer/template. These movements bring substrate and metal ions into precise geometrical arrangement for efficient catalysis. Arg258, no longer in salt bridge contact with Asp192, moves away from the active site and interacts with Glu295 and Tyr296 of the thumb subdomain pulling the thumb over the palm subdomain which stabilizes an active conformation of pol β.

ACKNOWLEDGMENT

We thank Dr. Robert Jackson for valuable discussions and continuing support.

REFERENCES

Arnold, E., Ding, J., Hughes, S. H., & Hostomsky, Z. (1995) *Curr. Opin. Struct. Biol. 5*, 27−38.
Beese, L. S., Derbyshire, V., & Steitz, T. A. (1993) *Science 260*, 352−355.
Boyer, P. L., Ferris, A. L., & Hughes, S. H. (1992) *J. Virol. 66*, 1031−1039.
Bryant, F. R., Johnson, K. A., & Benkovic, S. J. (1983) *Biochemistry 22*, 3537−3546.
Carson, M. (1991) *J. Appl. Crystallogr. 24*, 958−961.
Date, T., Yamamoto, S., Tanihara, K., Nishimoto, Y., & Matsukage, A. (1991) *Biochemistry 30*, 5286−5292.
Davies, J. F., II, Almassy, R. J., Hostomska, Z., Ferre, R., & Hostomsky, Z. (1994) *Cell 76*, 1123−1133.
Delarue, M., Poch, O., Tordo, N., Moras, D., & Argos, P. (1990) *Protein Eng. 3*, 461−467.
Dianov, G., Price, A., & Lindahl, T. (1992) *Mol. Cell. Biol. 12*, 1605−1612.
Hostomsky, Z., Appelt, K., & Ogden, R. C. (1989) *Biochem. Biophys. Res. Commun. 161*, 1056−1063.
Hostomsky, Z., Hostomska, Z., Fu, T.-B., & Taylor, J. (1992) *J. Virol. 66*, 3179−3192.
Jacobo-Molina, A., Ding, J., Nanni, R. G., Clark, A. D., Jr., Lu, X., Tantillo, C., Williams, R. L., Kamer, G., Ferris, A. L., Clark, P., Hizi, A., Hughes, S. H., & Arnold, E. (1993) *Proc. Natl. Acad. Sci. U.S.A. 90*, 6320−6324.
Jäger, J., Smerdon, S. J., Wang, J., Boisvert, D. C., & Steitz, T. A. (1994) *Structure 2*, 869−876.
Johnson, K. A. (1993) *Annu. Rev. Biochem. 62*, 685−713.
Kohlstaedt, L. A., Wang, J., Freidman, J. M., Rice, P. A., & Steitz, T. A. (1992) *Science 256*, 1783−1790.
Kumar, A., Abbotts, J., Karawya, E. M., & Wilson, S. H. (1990a) *Biochemistry 29*, 7156−7159.
Kumar, A., Widen, S. G., Williams, K. R., Kedar, P., Karpel, R. L., & Wilson, S. H. (1990b) *J. Biol. Chem. 265*, 2124−2131.
Larder, B. A., Purifoy, D. J., Powell, K. L., & Darby, G. (1987) *Nature 327*, 716−717.
Matsukage, A., Nishikawa, K., Ooi, T., Seto, Y., & Yamaguchi, M. (1987) *J. Biol. Chem. 262*, 8960−8962.
Matsumoto, Y., & Bogenhagen, D. F. (1989) *Mol. Cell. Biol. 9*, 3750−3757.
Matsumoto, Y., & Kim, K. (1995) *Science 269*, 699−702.
Mead, D. A., Szczesna-Skorupa, E., & Kemper, B. (1986) *Protein Eng. 1*, 67−74.

Ollis, D., Brick, P., Hamlin, R., Xuong, N. G., & Steitz, T. A. (1985) *Nature 313*, 762−766.

Pelletier, H., Sawaya, M. R., Kumar, A., Wilson, S. H., & Kraut, J. (1994) *Science 264*, 1891−1903.

Polesky, A. H., Steitz, T. A., Grindley, N. D. F., & Joyce, C. M. (1990) *J. Biol. Chem. 265*, 14579−14591.

Polesky, A. H., Dahlberg, M. E., Benkovic, S. J., Grindley, N. D. F., & Joyce, C. M. (1992) *J. Biol. Chem. 267*, 8417−8428.

Sawaya, M. R., Pelletier, H., Kumar, A., Wilson, S. H., & Kraut, J. (1994) *Science 264*, 1930−1935.

SenGupta, D. N., Zmudzka, B. Z., Kumar, P., Cobianchi, F., Skowronski, J., & Wilson, S. H. (1986) *Biochem. Biophys. Res. Commun. 136*, 341−347.

Sousa, R., Chung, Y. J., Rose, J. P., & Wang, B. C. (1993) *Nature 364*, 593−599.

Steitz, T. A., & Steitz, J. A. (1993) *Proc. Natl. Acad. Sci. U.S.A. 90*, 6498−6502.

Tanabe, K., Bohn, E. W., & Wilson, S. H. (1979) *Biochemistry 18*, 3401−3406.

Wang, T. S.-F. (1991) *Annu. Rev. Biochem. 60*, 513−552.

Wang, T. S.-F., Eichler, D. C., & Korn, D. (1977) *Biochemistry 16*, 4927−4934.

Wiebauer, K., & Jiricny, J. (1990) *Proc. Natl. Acad. Sci. U.S.A. 87*, 5842−5845.

Zmudzka, B. Z., SenGupta, D., Matsukage, A. Cobianchi, F., Kumar, P., & Wilson, S. H. (1986) *Proc. Natl. Acad. Sci. U.S.A. 83*, 5106−5110.

BI951968O